Laser & Photonics Reviews / Early View / 2300016

Research Article | Full Access

Electron Trapping Optical Storage Using A Single-Wavelength Light Source for Both Information Write-In and Read-Out

Chuan Liao, Hao Wu, Huajun Wu, Liangliang Zhang, Guo-hui Pan, Zhendong Hao, Feng Liu, Xiao-jun Wang, Jiahua Zhang

First published: 08 April 2023
https://doi.org/10.1002/lpor.202300016

Get it @ NYU

Abstract

In conventional electron trapping optical storage phosphor, both short- and long-wavelength light are needed for information write-in and read-out, respectively, complicating the optical storage system. Here, a $Y_3Al_2Ga_3O_{12}:Pr^{3+},Eu^{3+}$ optical storage phosphor with Pr^{3+} as an electron donor and Eu^{3+} as an electron trap is designed, and a single wavelength write-read scheme is demonstrated, which employs the same blue laser diode (LD) light source for both optical write-in through two-photon up-conversion charging and for read-out based on photostimulated luminescence (PSL), originated from $4f^15d^1 \rightarrow 4f^2$ transition of Pr^{3+} peaked at 315 nm in UV region. A deep electron trap with the mean depth of 1.42 eV and a narrow distribution of 0.3 eV is observed in the presence of Eu^{3+} in $Y_3Al_2Ga_3O_{12}:Pr^{3+}$, implying its long-term storage potential. The write-in and read-out experiments are conducted using 450 nm blue LD light with the power density of 1 W cm^{-2} for write-in and that with a low power density of 0.02 W cm^{-2} for read-out in order to avoid the effect of up-conversion luminescence on PSL signal. These results will advance the electron trapping optical storage scheme.

1 Introduction

Electron trapping phosphors have been extensively studied for their potential application in optical storage technique.[1-5] X-rays[6-9] or UV light[10-12] are typically used for information write-in through photoionization of activator followed by electron trapping, also called optical charging.[13-15] In the process of information read-out, the light with low-energy photons, such

as visible[16, 17] or near-infrared light,[18, 19] are used to release the trapped electrons to produce photostimulated luminescence (PSL) as a read-out signal.[20, 21] As a result, two wavelengths are needed for optical write-in and read-out in conventional electron trapping materials, which complicate the optical storage system.

Up-conversion charging (UCC)[22, 23] enables low-energy photons instead of UV photons to complete information write-in and it thus allows a single long-wavelength light with different intensities to serve both write-in and read-out. In UCC, the photoionization of activator is realized via multi-step excitation.[24] Trivalent praseodymium ion (Pr^{3+}) is a typical activator that can be photo-ionized to Pr^{4+}[25, 26] through two blue-photon excitation due to its unique energy level structure.[27-29] $Y_3Al_2Ga_3O_{12}:Pr^{3+}$ (YAGG:Pr^{3+}) has been found to show excellent blue light UCC followed by electron trapping.[30] However, the inherent traps in YAGG:Pr^{3+} are shallow with the thermoluminescence (TL) peaked at a low temperature of 325 K, limiting storage time. Hence, the introduction of deep electron traps in YAGG:Pr^{3+} is necessary to improve storage performance. It has been reported that Eu^{3+} in $Y_3Al_5O_{12}$ (YAG) can act as deep traps to capture electrons.[26] In view of the similar physical properties of YAGG and YAG garnets, it is expected that Eu^{3+} could also create deep electron traps in YAGG.

In this work, we have designed Pr^{3+} and Eu^{3+} co-doped YAGG optical storage phosphor and demonstrate a single wavelength write-read scheme using only blue laser diode (LD) light. The two-photon UCC for write-in and one-photon PSL for read-out are studied as a function of blue laser power density. The influence of up-conversion luminescence (UCL) on PSL is analyzed. The demonstration experiment of encoding and decoding binary information confirms the feasibility of the scheme. Moreover, electron traps with the mean depth of 1.42 eV and a narrow distribution of 0.3 eV are induced by co-doping Eu^{3+}, which guarantees long-term data storage. Our research is expected to push the further development of electron-trapping-based optical storage technique.

2 Results and Discussion

Design of Blue Light Write-Read Scheme

The photoluminescence excitation (PLE) spectrum of Pr^{3+} $^3P_0$ emission in YAGG:Pr^{3+},Eu^{3+} has one excitation band in the UV region (30 000–40 000 cm^{-1}) and four excitation lines in the visible region (20 000–24 000 cm^{-1}, corresponding to 500–430 nm), which are assigned to the $^3H_4 \rightarrow 4f^15d^1$ and $^3H_4 \rightarrow {}^3P_J$ (J = 0, 1, 2), $^1I_6$ transitions of Pr^{3+}, respectively (see **Figure** 1a).[31, 32] In our previous study, we used these ^3P_J, $^1I_6$ levels as intermediate energy levels to realize UCC in terms of electron trapping.[30] These levels match well with the emission wavelength of commercial blue LD (see Figure S1, Supporting Information), indicating that blue LD enables UCC instead of one-photon UV charging. As a result, we propose an optical write-read scheme

using only a single blue LD to simplify the optical storage system (see Figure 1b). The read-out process is performed through detecting PSL stimulated by the blue LD light. The PSL contains the $4f^15d^1 \rightarrow 4f^2$ emission band (280–450 nm) and the $4f^2 \rightarrow 4f^2$ emission lines of Pr^{3+}, as shown in the photoluminescence (PL) spectrum in Figure 1c. In fact, only the $4f^15d^1$ emission band is collected as the PSL signal because the $4f^2 \rightarrow 4f^2$ emissions also contain nonnegligible PL component that can be directly excited by the blue LD light through $^3H_4 \rightarrow {}^3P_J$, $^1I_6$ transitions.

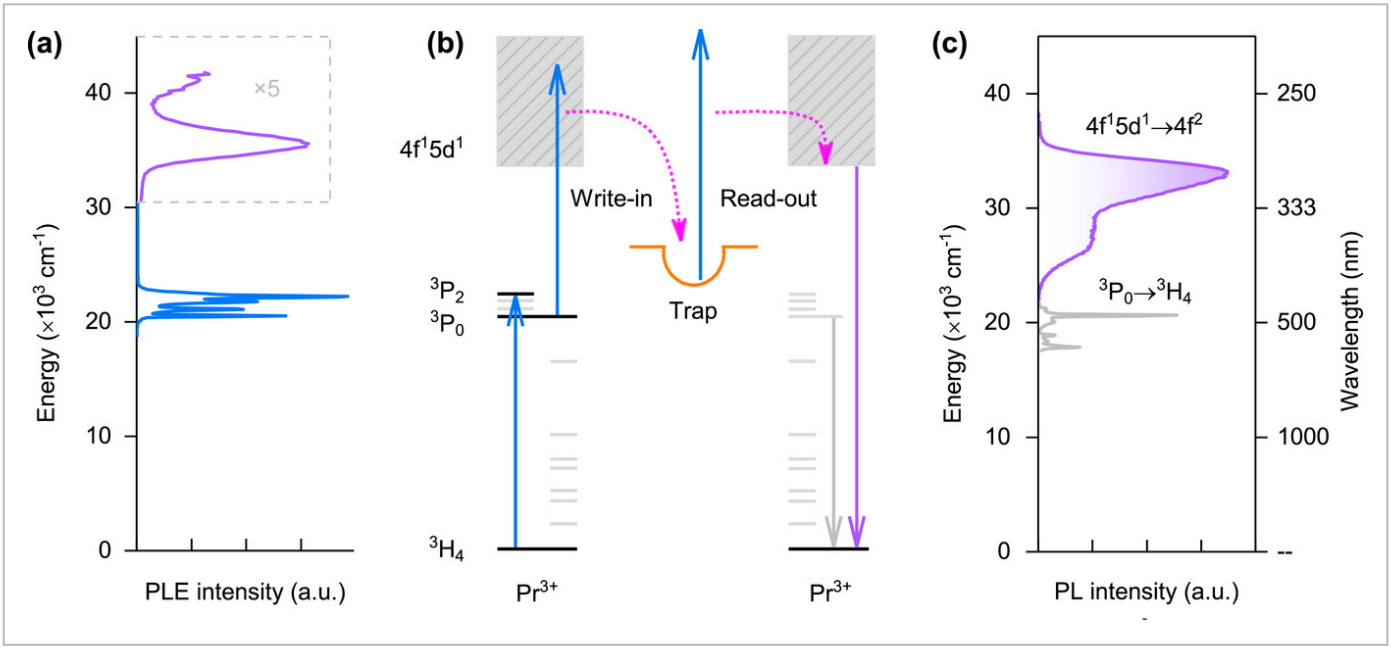

Figure 1

Open in figure viewer | PowerPoint

Single wavelength information write-read scheme based on Pr^{3+} energy level structure. a) PLE spectrum of YAGG:Pr^{3+},Eu^{3+} monitored at 562 nm. b) Schematic illustration of two blue-photon UCC for information write-in and one blue-photon PSL for information read-out. c) PL spectrum of YAGG:Pr^{3+},Eu^{3+} under 240 nm excitation.

Two-Photon UCC-Based Write-In

A 450 nm blue LD is used as an irradiation source to fill traps through UCC in YAGG:Pr^{3+},Eu^{3+} phosphor. To verify the multi-photon process of the UCC, the dependence of the number of filled traps on irradiation power density is studied. We use the integrated TL intensity to characterize the number of filled traps. Before charging at each irradiation power density, the phosphor is pre-heated at 723 K for 5 min to completely empty out the traps and subsequently cooled down to room temperature for achieving uncharged phosphor. The charging duration is limited to 15 s to ensure that the filled traps much less than the total traps, that is, far away from filling saturation. **Figure** 2a shows the TL glow curves of YAGG:Pr^{3+},Eu^{3+} after irradiation with different power densities. The curves continuously grow up with the increase of irradiation power density, indicating continuously increased filled traps. The integrated intensity of TL, I_{TL},

can be treated as the number of filled traps. The dependence of I_{TL} on irradiation power density, P, shows a nearly quadratic dependence (see Figure 2b), described as $I_{TL} \propto P^{1.78}$, indicating a two-photon UCC-based write-in (see Figure S2, Supporting Information).[28]

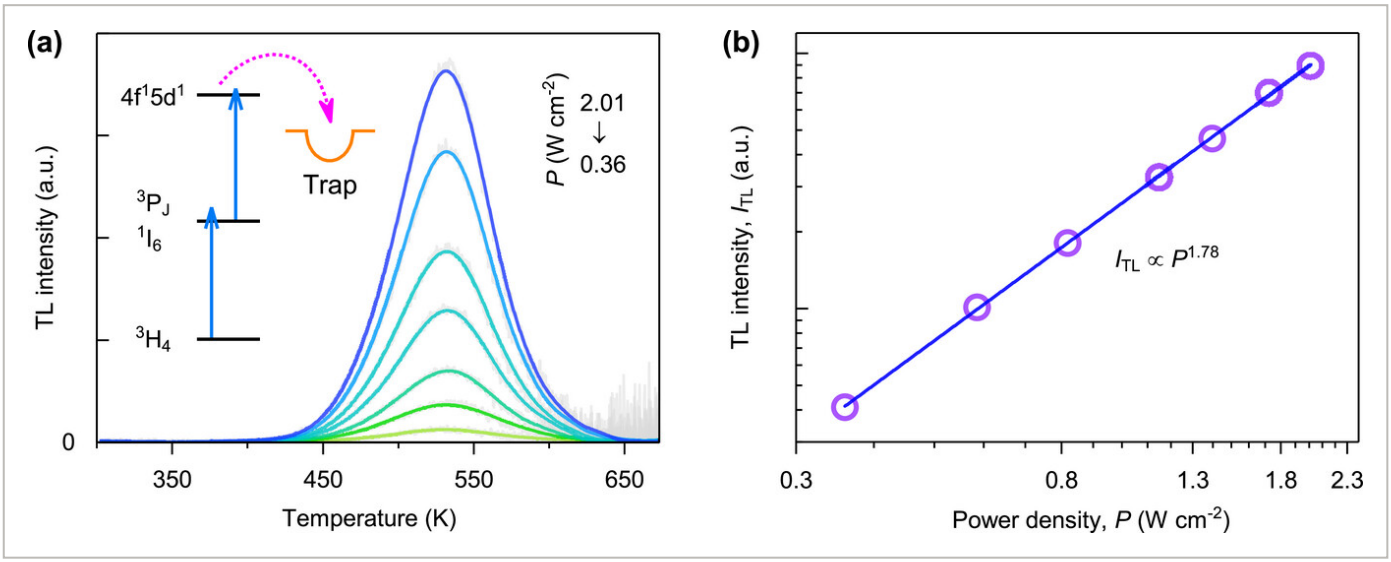

Figure 2

Open in figure viewer | PowerPoint

Verification of two blue-photon UCC for information write-in. a) TL glow curves in YAGG:Pr^{3+},Eu^{3+} after 450 nm irradiation with different power densities (heating rate: 1 K s^{-1}). The insert illustrates the processes of two-photon UCC. b) Integrated TL intensity versus irradiation power density.

One-Photon PSL-Based Read-Out

The information read-out scheme is based on the detection of PSL. To achieve photostimulation spectrum of a charged YAGG:Pr^{3+},Eu^{3+} phosphor is key to selection of efficient stimulation wavelength. Here, the charged phosphor is achieved through UCC by 450 nm blue LD light irradiation at 1 W cm^{-2} for 5 min. The photostimulation spectrum is obtained, as shown in **Figure** 3a. The visible monochromatic light from a filtered xenon arc lamp is used as a color tunable stimulation light (see Figure S3a, Supporting Information) and the PSL is monitored at 315 nm responsible for the $4f^15d^1 \rightarrow 4f^2$ emission band of Pr^{3+} in the UV range (see Figure 3b). The obtained photostimulation spectrum shows a wide band covering 420–650 nm region with a strong response to 450 nm blue LD light (see Figure 3a). The photostimulation spectral dip at 450 nm is due to the absorption of some stimulation light by the ^3P_J and $^1I_6$ energy levels, as shown in Figure S3b,c (Supporting Information).

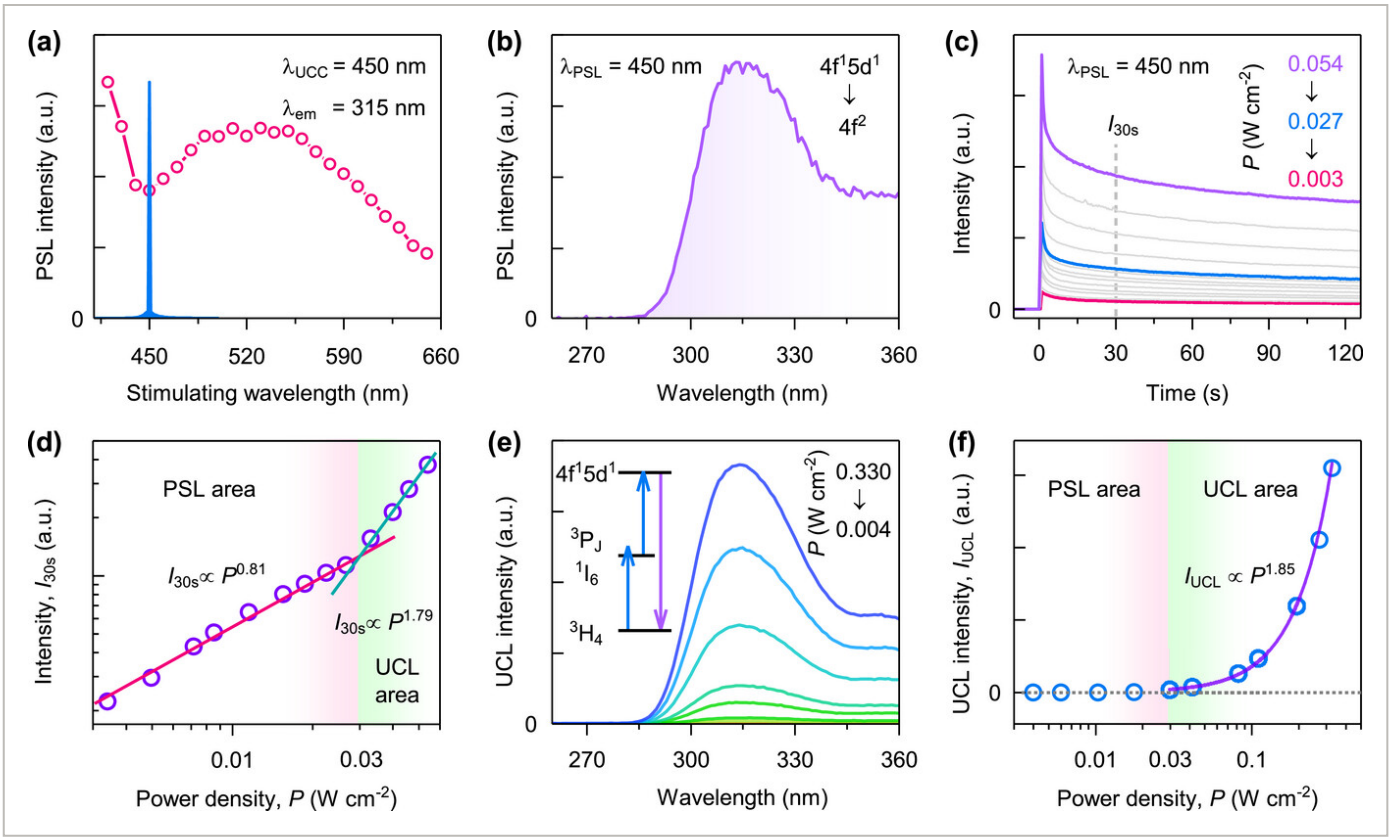

Figure 3

Open in figure viewer | PowerPoint

Read-out luminescence in YAGG:Pr^{3+}, Eu^{3+} stimulated by a 450 nm blue LD. a) Photostimulation spectrum and b) PSL spectrum. c) Luminescence decay curves monitored at 315 nm under different photostimulation power densities after UCC for 5 min at 1 W cm^{-2} irradiation density. d) Luminescence intensity (I_{30s}) versus the photostimulation power density. e) UCL spectra at different excitation power densities for the uncharged sample. The insert illustrates the process of two-photon UCL. f) The dependence of UCL intensity on excitation power density.

Upon 450 nm blue LD continuous stimulation, the charged phosphor shows a decay of the $4f^15d^1$ emission intensity with stimulation time, as shown in Figure 3c, reflecting the effect of stimulated detrapping process. The emission intensities at the stimulation time of 30 s in the decay curves, I_{30s}, are recorded as a function of the stimulation light power density, P, as shown in Figure 3d. One can see a linear dependence ($I_{30s} \propto P^{0.81}$) for stimulation light power density below 0.03 W cm^{-2} and a nearly quadratic dependence ($I_{30s} \propto P^{1.79}$) for stimulation light power density over 0.03 W cm^{-2}. The linear dependence is naturally the effect of one-photon PSL. The quadratic dependence is attributed to the effect of UCL. Indeed, the up-converted $4f^15d^1$ emissions are observed in an uncharged YAGG:Pr^{3+},Eu^{3+} phosphor under different excitation power densities, as shown in Figure 3e. From the UCL spectra, a nearly quadratic dependence of the integrated UCL intensity (I_{UCL}, 280–360 nm) on P is achieved, expressed as $I_{UCL} \propto P^{1.85}$ (see Figure 3f). From Figure 3f, the UCL is notable for excitation power density >0.03 W cm^{-2},

that is consistent with the result shown in Figure 3d. Hence, the stimulation density for suppressing UCL and achieving high-purity PSL-based read-out signal should be set <0.03 W cm^{-2}. Based on the results mentioned above, 1 and 0.02 W cm^{-2} power densities are selected for two-photon write-in and one-photon read-out, respectively, using only a single blue LD. Experiment results with one-time write-in and multiple time read-out are shown in Figure S4 (Supporting Information).

Eu^{3+} Induced Deep Traps

Deep electron traps are needed in Pr^{3+} singly doped YAGG for long-term optical information storage. According to the vacuum referred binding energy (VRBE) diagram,[33-38] Eu^{3+} can act as deep electron traps (see **Figure** 4a). Such a deduction has been verified by introducing Eu^{3+} in YAG garnet phosphor.[26] As a result, we design Pr^{3+} and Eu^{3+} codoped YAGG. Figure 4b shows the TL glow curves of Pr^{3+} singly doped YAGG and Pr^{3+}, Eu^{3+} codoped YAGG. It is apparent that the Pr^{3+} singly doped YAGG shows a main TL peak at 325 K, only slightly above room temperature, and the codoped YAGG shows a high temperature TL peak at 535 K, implying the creation of a deep electron trap and a long-term optical storage potential.

Figure 4

Open in figure viewer | PowerPoint

Mechanism of Eu^{3+} induced deep traps. a) The VRBE diagram of divalent (Ln^{2+}) and trivalent (Ln^{3+}) lanthanide ions in the $Y_3Al_2Ga_3O_{12}$ host. b) TL glow curves of YAGG:Pr^{3+} and YAGG:Pr^{3+},Eu^{3+}.

The depth distribution and storage time of traps are important indicators to evaluate the optical storage performance of the material. A series of TL glow curves of YAGG:Pr^{3+},Eu^{3+} were measured using the initial rise analysis method,[39, 40] as shown in **Figure** 5a. Since the population of UCC intermediate levels (^3P_J and $^1I_6$) are significantly affected by temperature (see Figure S5, Supporting Information), we improved the experimental design of the method to ensure the same results for each charging (see Figure S6, Supporting Information). The peak temperature of TL glow curve increases gradually with the rise of thermal cleaning temperature in Figure 5a, indicating that the traps have a continuous depth distribution.[41, 42] The initial rise analysis reveals that the traps are mainly distributed between 1.2 and 1.5 eV below the bottom of the conduction band, with the maximum traps density at 1.38 eV (see Figure 5b; Figure S7, Supporting Information). The deep and narrow traps are suitable for long-term storage and effective read-out of information.

Figure 5

Analysis of traps depth distribution and storage time. a) TL glow curves of YAGG:Pr^{3+},Eu^{3+} after undergoing different thermal cleaning temperatures (heating rate: 1 K s^{-1}). b) Relationship between traps depth and density. The horizontal axis is a discrete distribution. c) TL glow curves of YAGG:Pr^{3+},Eu^{3+} in different heating rates β. d) Heating rate plot of YAGG:Pr^{3+},Eu^{3+}.

The storage time, τ, can be calculated using the Arrhenius law given as[43, 44]

$$\tau = S^{-1}\exp\left(\frac{E}{kT}\right) \tag{1}$$

where S (s^{-1}) is the frequency factor, E (eV) is the depth of the traps, k (eV K^{-1}) is the Boltzmann constant, and T (K) is the storage ambient temperature. The peak position of the TL glow curves in Figure 2a does not vary with excitation power density, indicating that TL obeys the first order kinetics.[23, 45] Therefore, S and E were calculated by employing the Hoogenstraaten method[46, 47]

$$\frac{\beta E}{kT_m^2} = S\exp\left(-\frac{E}{kT_m}\right) \tag{2}$$

where β (K s^{-1}) is the heating rate, and T_m (K) is the peak temperature of the TL glow curve. The TL glow curves at different heating rates are shown in Figure 5c. The $\ln\left(T_m^2/\beta\right)$ versus $1/(kT_m)$ is plotted in Figure 5d. From the slope and intercept of the linear fit in Figure 5d, 1.42 eV for E and 1.61×10^{12} s^{-1} for S are determined. Using Equation (1), the room temperature (300 K) storage time is calculated to be as long as 1.24×10^{8} h, which implies an excellent long-term storage performance. In addition, the depths of the traps calculated by the initial rise analysis (1.38 eV) and Hoogenstraaten (1.42 eV) methods are in good agreement, indicating that the results are reliable. The difference of ≈0.5 eV between the two calculations and the predicted value of the VRBE diagram (see Figure 4a) can be attributed to three reasons: 1) VRBE diagram and TL method have systematic errors; 2) the bandgap of the material decreases with increasing temperature; and 3) the doping may affect the position of the bottom of the conduction band.[26]

Application for Optical Information Storage

To verify the feasibility of the optical write-in and read-out scheme and the storage performance of YAGG:Pr^{3+},Eu^{3+}, we demonstrate the binary information encoding and

decoding using only one blue LD. The experimental setup is shown in **Figure** 6a. The camera with a sensitive wavelength (308–321 nm) matching the PSL wavelength is used to record the decoding information, as shown in Figure 6b. We convert six decimal numbers to binary, with each line representing one decimal number (see Figure 6c). The binary information is written into a 6 × 6 YAGG:Pr^{3+},Eu^{3+} phosphor disks array by a two-photon UCC process (λ_{UCC} = 450 nm, 1 W cm^{-2}), as shown in Figure 6d. No UV afterglow is detected in the dark at room temperature after write-in (see Figure 6e), indicating that the traps are deep enough to suppress thermal release of trapped electrons at room temperature. When the phosphor disks are stimulated by 0.02 W cm^{-2} 450 nm LD light, the read-out information is well reproduced using an UV camera to detect the PSL signal (see Figure 6f). These results show the feasibility of our scheme as well as the potential long-term storage performance of YAGG:Pr^{3+},Eu^{3+}.

Figure 6

Open in figure viewer | PowerPoint

Demonstration experiment for single wavelength information write-read scheme. a) Schematic diagram of the experimental setup. b) PSL spectrum of YAGG:Pr^{3+},Eu^{3+} and sensitivity spectrum of the UV camera. c) Designed binary code array to be written in. d) Photograph of the phosphor disk array under natural light. e) Photograph of phosphor disk array taken in dark after two-photon write-in at room temperature. f) Photograph of reproduced array pattern taken in dark during one-photon read-out.

3 Conclusion

In summary, we have designed YAGG:Pr^{3+},Eu^{3+} electron trapping optical storage phosphor with Pr^{3+} as an electron donor and Eu^{3+} as an deep electron trap. A single wavelength write-read scheme is realized in YAGG:Pr^{3+},Eu^{3+}, which employs the same blue laser LD light source for both optical write-in through two-photon UCC and for read-out based on PSL, originated from $4f^15d^1 \rightarrow 4f^2$ transition of Pr^{3+} peaked at 315 nm in UV region. The UCC is the photoionization of Pr^{3+} via two-photon excitation followed with electron trapping by Eu^{3+}. The Pr^{3+}-Eu^{3+} donor–acceptor pair dominates the generation of deep electron traps with a mean depth of 1.42 eV and a narrow distribution of 0.3 eV, providing a long-term storage potential. The encoding and decoding experiment is conducted using 450 nm blue LD light. The laser power density for read-out should be low enough in order to avoid the effect of UCL on PSL signal. This work not only develops an excellent deep-trap storage material, but also opens a new way to simplify optical storage systems.

4 Experimental Section

Materials and Synthesis

A series of $(Y_{1-x-y}Pr_xEu_y)_3Al_2Ga_3O_{12}$ (x = 0–0.01; y = 0–0.01) storage phosphors with well-crystallinity was synthesized using the traditional high-temperature solid-phase method (see Figure S8, Supporting Information). The starting high purity raw materials of Y_2O_3 (99.99%), Al_2O_3 (99.99%), Ga_2O_3 (99.99%), $Pr(NO_3)_3$ (Pr^{3+} 0.1 mol L^{-1}), Eu_2O_3 (99.99%), and flux of 5 mol% H_3BO_3(A.R.) were weighed according to the stoichiometric ratio. All the raw materials were thoroughly ground in an agate mortar for 30 min. The mixture was pressed into a disk of 1 cm diameter and calcined in a muffle furnace in air at 1500 °C for 3 h. The scanning electron microscope (SEM) photographs showed that these phosphor particles were irregularly shaped and agglomerated, with single particle sizes ranging from 0.5 to 2 μm(see Figure S9, Supporting Information). In this work, the focus is co-doped sample $(Y_{0.999}Pr_{0.0005}Eu_{0.0005})_3Al_2Ga_3O_{12}$ (YAGG:Pr^{3+},Eu^{3+}).

Characterization and Measurements

The phase purity and crystal structure of all the samples were characterized by powder X-ray diffractometry (XRD) using Bruker AXS D8 scanning from 10° to 80° with Cu Kα radiation (λ = 0.15405 nm) at a rate of 0.2° per second at 40 kV and 30 mA. The particle size and morphology were measured by field emission SEM (Hitachi S-4800). The photoluminescence excitation (PLE) spectra, up-conversion luminescence (UCL) spectra, photostimulated luminescence (PSL) spectra, thermoluminescence (TL) glow curves, and PSL decay curves were measured using a FLS920 spectrometer with a 450 W xenon lamp (Edinburg Instruments, UK). The photoluminescence (PL) spectra in room temperature were recorded by using a charge-coupled device (CCD) spectrometer (QEPro, Ocean Optics, USA). The variable temperatures were obtained using an external heating/cooling stage (THMS-600, Linkam, UK). TL glow curves were measured by monitoring the $^3P_0 \rightarrow {}^3H_4$ (487 nm) emission of Pr^{3+} and the thermal quenching correction was performed (see Figure S5, Supporting Information). The uncharged phosphor was obtained by heating the phosphor at 723 K for 5 min to completely empty out the traps. A 450 nm blue laser diode (LD, LSR455CP-FC-12 W and LSR-PS-FA, Lasever Inc, China) with variable power density was used for up-conversion charging (UCC) and PSL. Information read-out images were taken using the Ofil Scalar UV camera (improved version), which was sensitive to 308 and 321 nm. During the information read-out, each binary cell was scanned point by point with a 0.02 W cm^{-2} 450 nm LD and the UV emission image (“Only UV” mode, marked purple) was recorded simultaneously. The images of all cells were spliced together to form Figure 6f.

Acknowledgements

This work was partially supported by the National Natural Science Foundation of China (Grant No. 11774046, 11904361, 11874055, and U22A20139), the Youth Innovation Promotion

Association CAS (No. 2020222), the Key Research and Development Program of Jilin Province (20200401050GX, 20200401004GX, and 20210201024GX), the Changchun Science and Technology Planning Project (Grant No. 21ZGY05), and the Opening Project Key Laboratory of Transparent Opto-functional Inorganic Material, Chinese Academy of Sciences.

Conflict of Interest

The authors declare no conflict of interest.

Open Research

Data Availability Statement

The data that support the findings of this study are available from the corresponding author upon reasonable request.

Supporting Information

Filename	Description
lpor202300016-sup-0001-SuppMat.pdf 558.3 KB	Supporting Information

Please note: The publisher is not responsible for the content or functionality of any supporting information supplied by the authors. Any queries (other than missing content) should be directed to the corresponding author for the article.

References

1 Y. Li, M. Gecevicius, J. Qiu, *Chem. Soc. Rev.* 2016, **45**, 2090.

2 J. Xu, S. Tanabe, *J. Lumin.* 2019, **205**, 581.

3 L. Yuan, Y. Jin, Y. Su, H. Wu, Y. Hu, S. Yang, *Laser Photon. Rev.* 2020, **14**, 2000123.

4 W. Li, Y. Zhuang, P. Zheng, T. Zhou, J. Xu, J. Ueda, S. Tanabe, L. Wang, R. Xie, *ACS Appl. Mater. Interfaces* 2018, **10**, 27150.

5 Y. Zhuang, L. Wang, Y. Lv, T. Zhou, R. Xie, *Adv. Funct. Mater.* 2018, **28**, 1705769.

6 U. Rogulis, I. Tale, T. Hangleiter, *J. Phys.: Condens. Matter* 1995, **7**, 3129.

7 A. Wiatrowska, E. Zych, *J. Phys. Chem. C* 2013, **117**, 11449.

8 Y. Zhuang, D. Chen, W. Chen, W. Zhang, X. Su, R. Deng, Z. An, H. Chen, R. Xie, *Light Sci. Appl.* 2021, **10**, 132.

9 Y. Yang, Z. Li, J. Zhang, Y. Lu, S. Guo, Q. Zhao, X. Wang, Z. Yong, H. Li, J. Ma, Y. Kuroiwa, C. Moriyoshi, L. Hu, L. Zhang, L. Zheng, H. Sun, *Light Sci. Appl.* 2018, **7**, 88.

10 D. C. Rodríguez Burbano, E. M. Rodríguez, P. Dorenbos, M. Bettinelli, J. A. Capobianco, *J. Mater. Chem. C* 2014, **2**, 228.

11 S. Lin, H. Lin, C. Ma, Y. Cheng, S. Ye, F. Lin, R. Li, J. Xu, Y. Wang, *Light Sci. Appl.* 2020, **9**, 22.

12 M. Deng, Q. Liu, Y. Zhang, C. Wang, X. Guo, Z. Zhou, X. Xu, *Adv. Opt. Mater.* 2021, **9**, 2002090.

13 S. Jutamulia, G. Storti, J. Lindmayer, W. Seiderman, *Appl. Optics* 1990, **29**, 4806.

14 M. Lastusaari, A. J. J. Bos, P. Dorenbos, T. Laamanen, M. Malkamäki, L. C. V. Rodrigues, J. Hölsä, *J. Therm. Anal. Calorim.* 2015, **121**, 29.

15 B. Wang, X. Li, Y. Chen, Y. Chen, J. Zhou, Q. Zeng, *J. Am. Ceram. Soc.* 2018, **101**, 4598.

16 F. Liu, W. Yan, Y. Chuang, Z. Zhen, J. Xie, Z. Pan, *Sci. Rep.* 2013, **3**, 1554.

17 Y. Liang, F. Liu, Y. Chen, X. Wang, K. Sun, Z. Pan, *Light Sci. Appl.* 2016, **5**, e16124.

18 S. Lin, H. Lin, Q. Huang, Y. Cheng, J. Xu, J. Wang, X. Xiang, C. Wang, L. Zhang, Y. Wang, *Laser Photon. Rev.* 2019, **13**, 1900006.

19 H. Bian, X. Qin, Y. Wu, Z. Yi, S. Liu, Y. Wang, C. D. S. Brites, L. D. Carlos, X. Liu, *Adv. Mater.* 2022, **34**, 2101895.

20 K. Takahashi, K. Kohda, J. Miyahara, Y. Kanemitsu, K. Amitani, S. Shionoya, *J. Lumin.* 1984, **31**, 266.

21 D. Liu, L. Yuan, Y. Jin, H. Wu, Y. Lv, G. Xiong, G. Ju, L. Chen, S. Yang, Y. Hu, *ACS Appl. Mater. Interfaces* 2019, **11**, 35023.

22 Y. Chen, F. Liu, Y. Liang, X. Wang, J. Bi, X. Wang, Z. Pan, *J. Mater. Chem. C* 2018, **6**, 8003.

23 F. Liu, Y. Liang, Z. Pan, *Phys. Rev. Lett.* 2014, **113**, 177401.

24 C. Li, X. Zhao, T. Guo, F. Liu, X. Wang, C. Liao, J. Zhang, *Acta Phys. Sin.* 2022, **71**, 077801.

25 F. You, A. J. Bos, Q. Shi, S. Huang, P. Dorenbos, *J. Phys. Condens. Matter* 2011, **23**, 215502.

26 F. You, A. J. J. Bos, Q. Shi, S. Huang, P. Dorenbos, *Phys. Rev. B* 2012, **85**, 115101.

27 S. Yan, Q. Gao, X. Zhao, A. Wang, Y. Liu, J. Zhang, X. Wang, F. Liu, *J. Lumin.* 2020, **226**, 117427.

28 S. Yan, F. Liu, J. Zhang, X. Wang, Y. Liu, *Phys. Rev. Appl.* 2020, **13**, 044051.

29 X. Zhao, C. Li, F. Liu, X. Wang, *J. Rare Earth.* 2021, **39**, 1492.

30 C. Liao, F. Chen, H. Wu, H. Wu, L. Zhang, G. Pan, F. Liu, X. Wang, J. Zhang, *J. Mater. Chem. C* 2022, **10**, 11884.

31 F. You, S. Huang, C. Meng, D. Wang, J. Xu, Y. Huang, G. Zhang, *J. Lumin.* 2007, **122**, 58.

32 B. Kahouadji, L. Guerbous, D. J. Jovanović, M. D. Dramićanin, *J. Lumin.* 2022, **241**, 118499.

33 P. Dorenbos, A. J. J. Bos, *Radiat. Meas.* 2008, **43**, 139.

34 P. Dorenbos, *Phys. Rev. B* 2012, **85**, 165107.

35 P. Dorenbos, *J. Lumin.* 2013, **135**, 93.

36 J. Ueda, P. Dorenbos, A. J. J. Bos, K. Kuroishi, S. Tanabe, *J. Mater. Chem. C* 2015, **3**, 5642.

37 J. Xu, J. Ueda, S. Tanabe, *J. Mater. Chem. C* 2016, **4**, 4380.

38 T. Lyu, P. Dorenbos, *Chem. Eng. J.* 2020, **400**, 124776.

39 C. Wang, Y. Jin, Y. Lv, G. Ju, D. Liu, L. Chen, Z. Li, Y. Hu, *J. Mater. Chem. C* 2018, **6**, 6058.

40 K. Van den Eeckhout, A. J. J. Bos, D. Poelman, P. F. Smet, *Phys. Rev. B* 2013, **87**, 045126.

41 S. W. S. McKeever, *Phys. Stat. Sol.* 1980, **62**, 331.

42 Y. Kitagawa, J. Ueda, S. Tanabe, *Phys. Status Solidi A* 2022, **219**, 2100670.

43 J. Zhang, M. Gecevičius, M. Beresna, P. G. Kazansky, *Phys. Rev. Lett.* 2014, **112**, 033901.

44 Z. Wang, W. Wang, H. Zhou, J. Zhang, S. Peng, Z. Zhao, Y. Wang, *Inorg. Chem.* 2016, **55**, 12822.

45 A. J. J. Bos, *Radiat. Meas.* 2006, **41**, S45.

46 W. Hoogenstraaten, *Philips Res. Rep.* 1958, **13**, 515.

47 J. Ueda, A. Hashimoto, S. Takemura, K. Ogasawara, P. Dorenbos, S. Tanabe, *J. Lumin.* 2017, **192**, 371.